RESEARCH NOTE

MAXIMUM ALLOWABLE LOAD ON WHEELED MOBILE MANIPULATORS

M. Habibnejad Korayem and H. Ghariblu

Department of Mechanical Engineering, Iran University of Science and Technology
Tehran, Iran, hkorayem@iust.ac.ir

(Received: February 9, 2002 – Accepted in Revised Form: May 15, 2003)

Abstract This paper develops a computational technique for finding the maximum allowable load of mobile manipulators for a given trajectory. The maximum allowable loads which can be achieved by a mobile manipulator during a given trajectory are limited by the number of factors; probably the dynamic properties of mobile base and mounted manipulator, their actuator limitations and additional constraints applied to resolving the redundancy are the most important factors. To resolve extra D.O.F introduced by the base mobility, additional constraint functions are proposed directly in the task space of mobile manipulator. Finally, in two numerical examples involving a two-link planar manipulator mounted on a differentially driven mobile base, application of the method to determining maximum allowable load is verified. The simulation results demonstrates the maximum allowable load on a desired trajectory has not a unique value and directly depends on the additional constraint functions which applies to resolve the motion redundancy.

Key Words Given Trajectory, Load Carrying Capacity, Base Replacement, Manipulator

چکیده در این مقاله روش محاسباتی تعیین حداکثر ظرفیت حمل بار بازوهای رباتی چرخ دار در یک مسیر مشخص بدست می آید. حرکت یک بازو با حداکثر بار قابل حمل یکی از معیارهای مهم در طراحی مسیر حرکت می باشد. عوامل متعددی می توانند ظرفیت حمل بار یک بازوی رباتی متحرک را تحت تأثیر قرار دهند. خواص دینامیکی پایه و بازو، محدودیت گشتاور موتورهای متحرک و قیدهای اضافی که برای حل مسئله درجات آزادی مازاد اعمال می گردند, از مهمترین عوامل تأثیر گذار در ظرفیت حمل بار سیستم تلقی می گردند. برای حل مسئله درجات مازاد اضافی که بواسطه حرکت پایه به سیستم تحلیل می گردند، قیدهایی به صورت توابع به معادله حرکت سیستم افزوده شده اند. در دو نمونه مثال عددی, یک بازوی دولینکی صفحه ای که روی یک پایه متحرک چرخ دار نصب شده است، برای نمایش کاربرد روش تعیین ظرفیت حمل بار استفاده شده و صحت الگوریتم مورد تحقیق قرار گرفته است. نتایج شبیه سازی بوضوح نشان می دهد که حداکثر بار مجاز قابل حمل در یک مسیر مشخص تابعی از نوع قیدهایی است که برای حل مسئله درجه آزاد اعمال می گردد و مقدار یکتایی ندارد.

1. INTRODUCTION

The maximum allowable load of a fixed base manipulator is often defined as the maximum payload that the manipulator can repeatedly lift in its fully extended configuration. However, to determine the maximum allowable load of a robot must take into account the inertia effect of the load along a desired trajectory as well as the manipulator dynamics. Wang and Ravani were shown the maximum allowable load of a fixed base manipulator on a given trajectory is primarily constrained by the joint actuator torque and its velocity characteristic [1]. Korayem and Basu by removing rigid body assumption for the links and joints imposed additional constraints as resultant end effector deflection for flexible manipulators [2-4]. They presented a method to determine maximum allowable load of flexible manipulators subject to both actuator and end effector deflection constraints. Carriker et. al. worked on determining point-to-point motions, which must perform a sequence of tasks defined by position, orientation, force and moment vectors of the end effector [5].

Papadopoulos and Gonthier considered the effect of base mobility of robotic manipulators on large force quasi-static tasks [6]. They introduced the force workspace concept for identifying proper base guaranteeing task execution along desired paths. In their work the dynamic effects of the load and manipulator are not examined. There are some other works, which published about carrying heavy loads and stability of the wheeled mobile manipulators [7-9]. Also there are some other research studies which consider the problem of large force task planning and carrying heavy loads on mobile manipulators, however non of them consider the problem of finding maximum load carrying capacity of mobile manipulators.

In this paper, we present a new method of determining the maximum allowable load for mobile manipulators subject to both actuator and redundancy constraints. For motion planning and redundancy resolution, additional constraint functions and the augmented Jacobian matrix are used. The recursive Newton-Euler method is used to formulate the dynamic effects of combined mobile base and manipulator motion on joint actuator torques. A general computational procedure is presented for finding the maximum allowable load of multi-link mobile manipulators for a desired trajectory. Finally, by numerical examples involving a two-link planar manipulator mounted on a differentially driven mobile base, application of the method is presented and simulation test is carried out.

2. KINEMATIC MODELING OF MOBILE MANIPULATORS

The position of the end effector in the task space of mobile manipulators can be defined as bellow:

$$X = X_b(q_b) + X_{m/b}(q_m) \tag{1}$$

where $X = [x \quad y \quad z]^T$ and $X_b = [x_b \quad y_b \quad z_b]^T$ are the position of the end effector and the base in the inertial reference frame. $X_{m/b} = [x_{m/b} \quad y_{m/b} \quad z_{m/b}]^T$ is the position vector of manipulator with respect to the base. The Jacobian equation of the mobile manipulator can be determined as:

$$\dot{X} = J\dot{q} \tag{2}$$

where $J = \begin{pmatrix} J_b & J_m \end{pmatrix}$ and $\dot{q} = (\dot{q}_b \quad \dot{q}_m)^T$. $\dot{X} \in R^m$ denotes the task velocity space of mobile manipulator with respect to the fixed coordinate frame and $\dot{q} \in R^n$ is the joints velocity space.

The general form of the constraint equations can be written as:

$$J_c\dot{q} = 0 \tag{3}$$

where $J_c \in R^{c \times n}$. On the other hand, the combined system of mobile manipulator has extra degrees of freedom on its motion. Therefore to resolving the redundancy, we can apply r additional constraint equations, which can be written as:

$$\dot{X}_Z = J_z\dot{q} \tag{4}$$

where $J_z \in R^{r \times n}$. Hence the kinematic equation of mobile manipulators by combining the Equations (2), (3) and (4) is written as:

$$\begin{pmatrix} \dot{X} & \dot{X}_z & 0 \end{pmatrix}^T = \begin{pmatrix} J & J_z & J_c \end{pmatrix}^T \dot{q} \tag{5}$$

Here $J_a = \begin{pmatrix} J & J_z & J_c \end{pmatrix}^T$ is named as augmented Jacobian matrix. The J_Z matrix can be obtained using singular value decomposition and other methods. However, the simple method is to choose user specified constraint equations in general form [10]:

$$X_Z = g(q) \tag{6}$$

By differentiating of Equation 6 with respect to time, we have $\dot{X}_z = J_z\dot{q}$ similar to Equation 4.

The augmented Jacobian matrix J_a, regardless of the configuration q of the mobile manipulator must be non-singular, or the determinant of J_a must be non-zero:

$$Det(J_a) \neq 0. \tag{7}$$

If the resultant J_a to be non-singular then joints velocity acceleration vectors are found:

$$\dot{q} = J_a^{-1}\begin{pmatrix} \dot{X} & \dot{X}_z & 0 \end{pmatrix}^T \tag{8}$$

$$\ddot{q} = J_a^{-1}(\begin{pmatrix} \ddot{X} & \ddot{X}_z & 0 \end{pmatrix}^T - \dot{J}_a \dot{q}) \tag{9}$$

3. DYNAMIC MODELING OF MOBILE MANIPULATORS

In order to obtain DLCC for a mobile manipulator, proper modeling of mobile manipulator and load dynamic is a prerequisite. Therefore the desired values are evaluated on the $(n+1)th$ coordinate system attached to the center of mass of the end-effector and load as a composite body [1]. The proposed algorithm is based upon the forward recursive Newton-Euler formulation that is used to determine the linear and angular accelerations of the ith link (ω_i and α_i) and its mass center (v_{ci} and a_{ci}) iteratively computed from link 1 out to link n. The dynamic equations are obtained using the Newton-Euler approach as follows:

$$F_i = ma_{ci} \tag{10}$$

$$N_i = {}^{ci}I\alpha_i + \omega_i \times {}^{ci}I\omega_i \tag{11}$$

where c_i is the coordinate frame has its origin at the center of the link and has the same orientation as the ith link coordinate frame. Then, the joint actuator torque's is computed recursively from link n back to link 1 by the backward Newton-Euler formulation as:

$${}^i f_i = {}_{i+1}^{i}R\, {}^{i+1}f_{i+1} + {}^iF_i \tag{12}$$

$${}^i n_i = {}^iN_i + {}_{i+1}^{i}R\, {}^{i+1}n_{i+1} + {}^iP_{ci} \times {}^iF_i + {}^iP_{i+1} \times {}_{i+1}^{i}R\, {}^{i+1}f_{i+1} \tag{13}$$

$$\tau_i = {}^i n_i^T\, {}^i z_i \tag{14}$$

Here ${}_{i+1}^{i}R$ describes the rotation matrix from coordinate frame $i+1$ relative to coordinate frame i. The other variables denoted by the general form ${}^i f_i$ describe the vector f in the ith link described in coordinate frame i. Also on the above formulation, f denotes joint force, n joint torque, P position vector, τ joint's actuator torque and z is the unit vector in the direction of joint's rotation axis.

4. DETERMINING MAXIMUM ALLOWABLE LOAD

For determining the maximum allowable load, separate computation of the actuators torque for compensating the load dynamics τ_l and the manipulator dynamics τ_{nl} on the each joint is needed. Therefore the mobile manipulator dynamic computations are executed in two steps. In both steps, by neglecting the load moment of inertia I_{load} and considering only mass portion of load, ${}^{n+1}n_{n+1}$ is set equal to zero in the dynamic equations. In the first step the total dynamic effects of the load and mobile manipulator on the actuators τ is considered and ${}^{n+1}f_{n+1}$ is set equal to $m_c(g - a_c)$, where m_c and a_c are of the end-effector and load masses and accelerations as a composite body and g is the gravitational acceleration vector. In the second step, ${}^{n+1}f_{n+1}$ is set equal to zero, which considers only the effect of the mobile manipulator dynamics on the joint actuators τ_{nl}. By subtracting τ_{nl} from τ, the τ_l is resulted:

$$\tau_l = \tau - \tau_{nl} \tag{15}$$

In this Section the computational procedure for determining the maximum allowable load is outlined and also flowcharted in Figure 1. Continuous trajectory of the end effector is discretized into equally spaced m points along the trajectory, and then the total torque on *jth* joint at each grid point $\tau_j(k)$ is obtained where $k = 1,2,...,m$. The joints actuator torque constraints are formulated based on the typical joint-speed characteristics of DC motors as follows:

$$T^{(+)} = k_1 - k_2 \dot{q}$$
$$T^{(-)} = -k_1 - k_2 \dot{q} \tag{16}$$

where $k_1 = T_s$ and $k_2 = T_s / \omega_{nl}$, T_s is the stall torque and ω_{nl} is the maximum no-load speed of the motor. If $\tau_{nl}(k)$ satisfies the following inequality:

$$T_j^{(+)}(k) \le \tau_{nl}(k) \le T_j^{(-)}(k) \tag{17}$$

and if

$$\left|T_j^{(+)}(k) - \tau_{nl}(k)\right| < \left|T_j^{(-)}(k) - \tau_{nl}(k)\right| \tag{18}$$

then the load coefficient at *jth* joint C_j can be calculated as bellow:

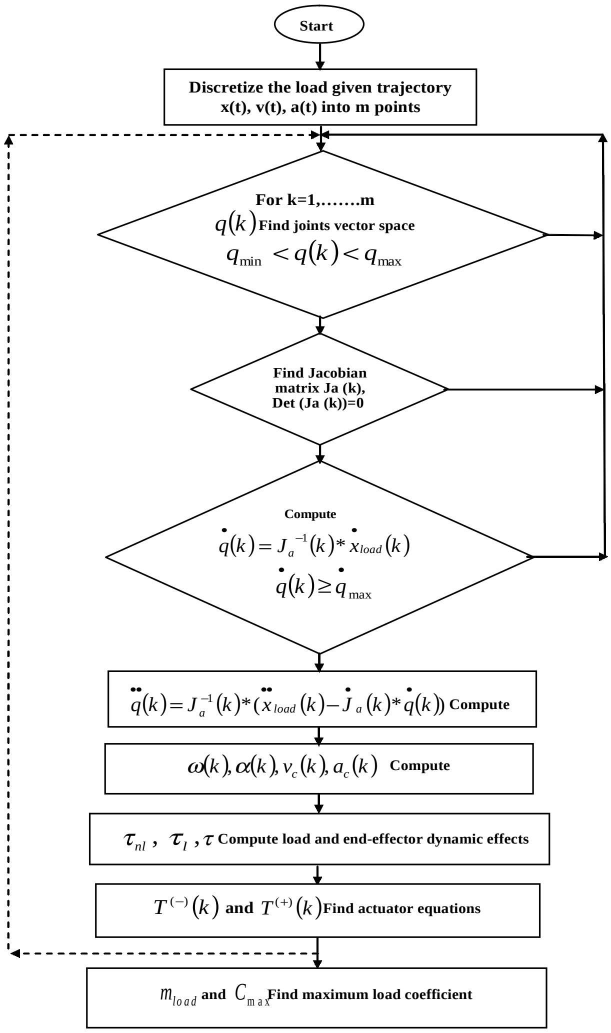

Figure 1. Flowchart of determining maximum allowable load.

$$C_j(k) = \left|T_j^{(+)}(k) - \tau_{nl}(k)\right| / \tau_l(k) \tag{19}$$

else, if Equation 18, is not satisfied then:

$$C_j(k) = \left|T^{(-)}(k) - \tau_{nl}(k)\right| / \tau_l(k) \tag{20}$$

otherwise, if $\tau_{nl}(k) > T^{(+)}(k)$ and $\tau_l(k) < 0$ then:

$$C_j(k) = \left|\ \tau_{nl}(k) - T^{(+)}(k) / \tau_l(k)\ \right| \tag{21}$$

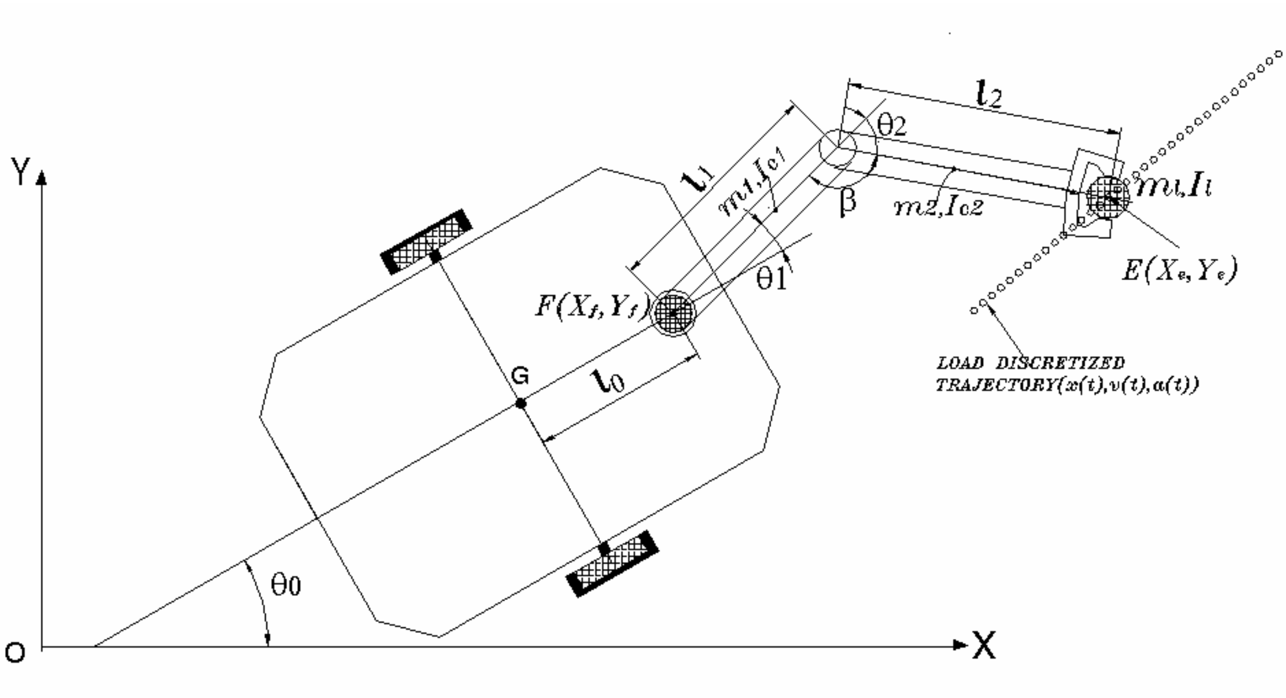

Figure 2. Schematic view of mobile manipulator.

Under the different conditions, unrealizable case encountered (e.g., if the desired speed is too high or the desired trajectory is physically impossible) and we have:

$$C_j(k) = 0 \tag{22}$$

The maximum load coefficient at the jth joint along the given trajectory is computed as:

$$C_{j,\max} = \min\{C_j(k), k = 1,2,...,m\} \tag{23}$$

Finally, the maximum load coefficient for the mobile manipulator $C_{\max}$ along the given trajectory is computed from

$$C_{\max} = \min\{C_{j,\max}, j = 1 \ \ to \ \ n\}. \tag{24}$$

where n is the number of manipulator's joint.

The maximum allowable load carrying capacity for the mobile manipulator is computed from the following equation:

$$m_{load} = C_{\max} \times m_l \tag{25}$$

5. SIMULATION STUDIES

To investigate the proposed algorithm, some simulation studies are presented. In these studies, a specified trajectory for the load is assumed. A two-link planar manipulator mounted on a differentially driven mobile base is considered as a case study (Figure 2). The joint actuators are similar and their constants are $\omega_{nl} = 3.5 rad/s$ and $k_1 = 63.22 N.m$. For simulation study two cases are considered in a situation where the same trajectory for the load is selected, but a different additional constraint

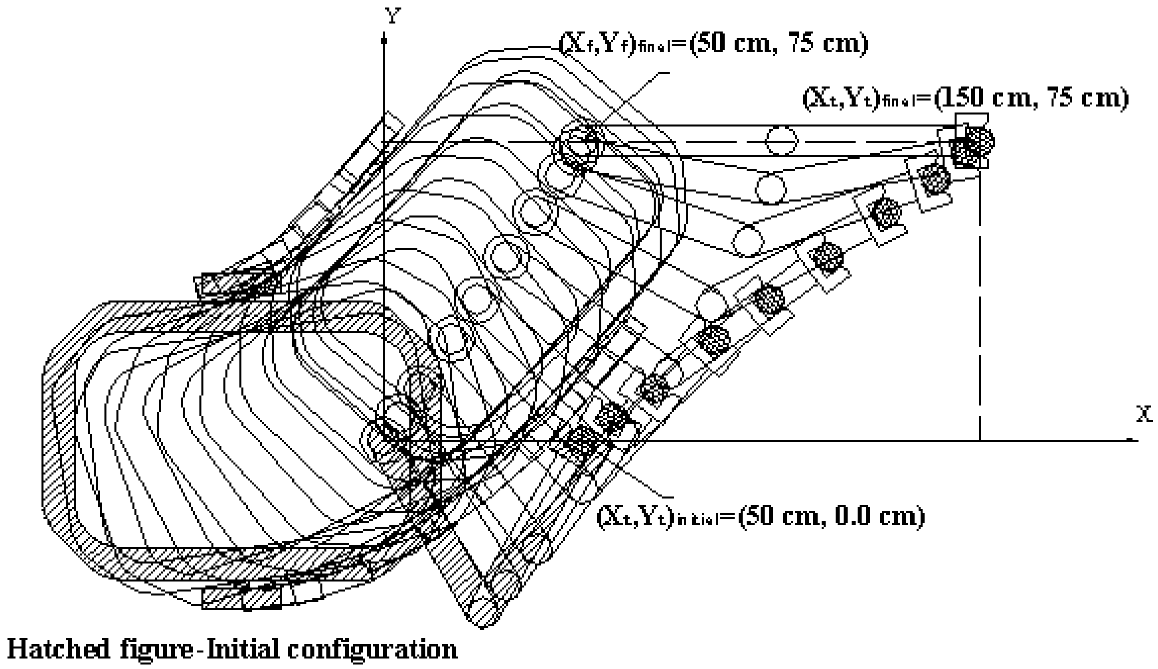

Figure 3. The movement of the mobile manipulator from initial to final configuration along the trajectory.

functions are applied to resolve the motion redundancy in each case.

5.1. Simulation Model-1 The planar two-link arm is mounted on mobile base at point F on the main axis of the base (Figure 2). The position of point F relative to world coordinate frame is denoted by x_f, y_f. In this case, the user specified additional constraints $X_z = g(q)$, are considered as the base position coordinates $F(x_f, y_f)$.

We combine the additional constraint Equations (A-3), the end effector velocity components Equations (A-4) and the nonholonomic constraint Equation (A-5) (please see Appendix A for details).

Then we rewrite these equations in the matrix form as mentioned in the Equation (5):

$$\begin{pmatrix} Sin(\theta_0) & -Cos(\theta_0) & l_0 & 0 & 0 \\ 1 & 0 & J_{23} & J_{24} & J_{25} \\ 0 & 1 & J_{33} & J_{34} & J_{35} \\ 1 & 0 & 0 & 0 & 0 \\ 0 & 1 & 0 & 0 & 0 \end{pmatrix} \begin{pmatrix} \dot{x}_f \\ \dot{y}_f \\ \dot{\theta}_0 \\ \dot{\theta}_1 \\ \dot{\theta}_2 \end{pmatrix} = \begin{pmatrix} 0 \\ \dot{x}_e \\ \dot{y}_e \\ \dot{x}_f \\ \dot{y}_f \end{pmatrix} \tag{26}$$

where, the expression of $J_{23}, J_{24}, J_{25}, J_{33}, J_{34}$ and J_{35} are given by:

$$J_{23} = J_{24} = -l_1 \sin(\theta_0 + \theta_1) - l_2 \sin(\theta_0 + \theta_1 + \theta_2),$$

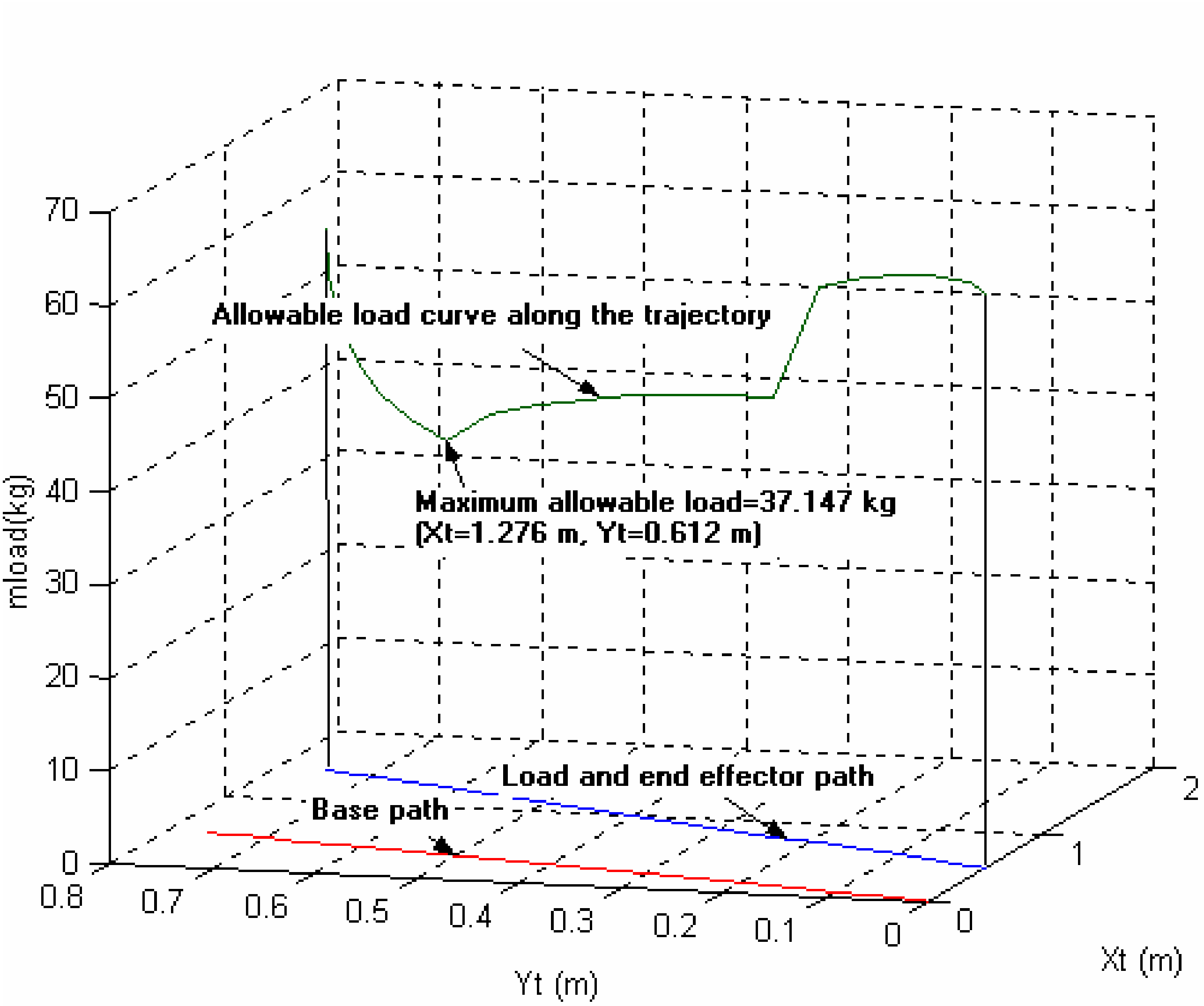

Figure 4. The variation of the allowable load along the load trajectory and associated with maximum allowable load.

$J_{25} = -l_2 \sin(\theta_0 + \theta_1 + \theta_2)$,

$J_{33} = J_{34} = l_1 \cos(\theta_0 + \theta_1) + l_2 \cos(\theta_0 + \theta_1 + \theta_2)$

and $J_{35} = l_2 \cos(\theta_0 + \theta_1 + \theta_2)$

By direct calculation, the determinant of the augmented Jacobian matrix on the left hand side of the Equation (26) is found

$$Det(J_a) = l_0 \times l_1 \times l_2 \sin(\theta_2)$$

Hence J_a is non-singular provided that $\theta_2 \neq 0^\circ$ *or* 180°. That is the two arms are not along the same axis. Suppose that the base length is $l_0 = 40$ cm, the links length are

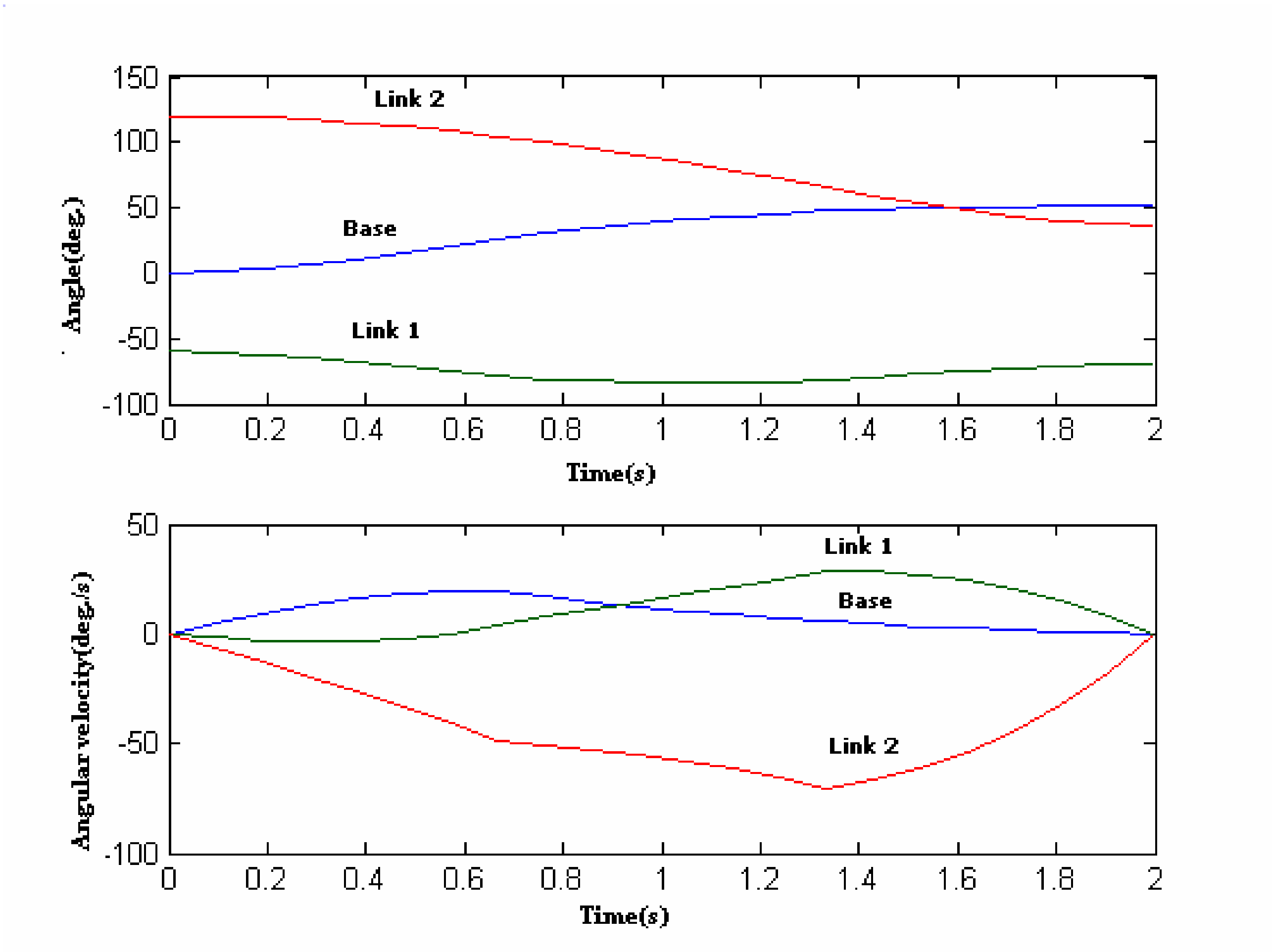

Figure 5. Variations of the base and links angles and angular velocities along the trajectory.

$l_1 = l_2 = 50 \quad cm$. Let the initial configuration of the mobile base is given by:

$$q_i = \{x_f, \quad y_f, \quad \theta_0\} = \{0 \quad cm, 0 \quad cm, 0 \quad rad\}$$

The initial task vector is considered as $X_i = \{x_t, y_t, x_f, y_f\}_i = \{50,0,0,0\}cm$ and desired final task vector at time $t = 2Sec$ is specified as $X_f = \{x_t, y_t, x_f, y_f\}_f = \{150,75,50,75\}cm$.

Notice that final tool tip position is not feasible without the base motion. The desired task space path is specified as straight lines from initial to final configuration. By simulation study the overall movement of the mobile manipulator is found and shown in Figure 3.

Using the recursive Newton–Euler's dynamic formulation the torques at the joints of the manipulator are obtained as follows:

$$\tau_1 = H_{11} \ddot{X}_f + H_{12} \ddot{Y}_f + H_{13} \dot{\omega}_2 + H_{14}\omega_2^2 + H_{15} \dot{\omega}_1 + H_{16}\omega_1^2 \tag{27}$$

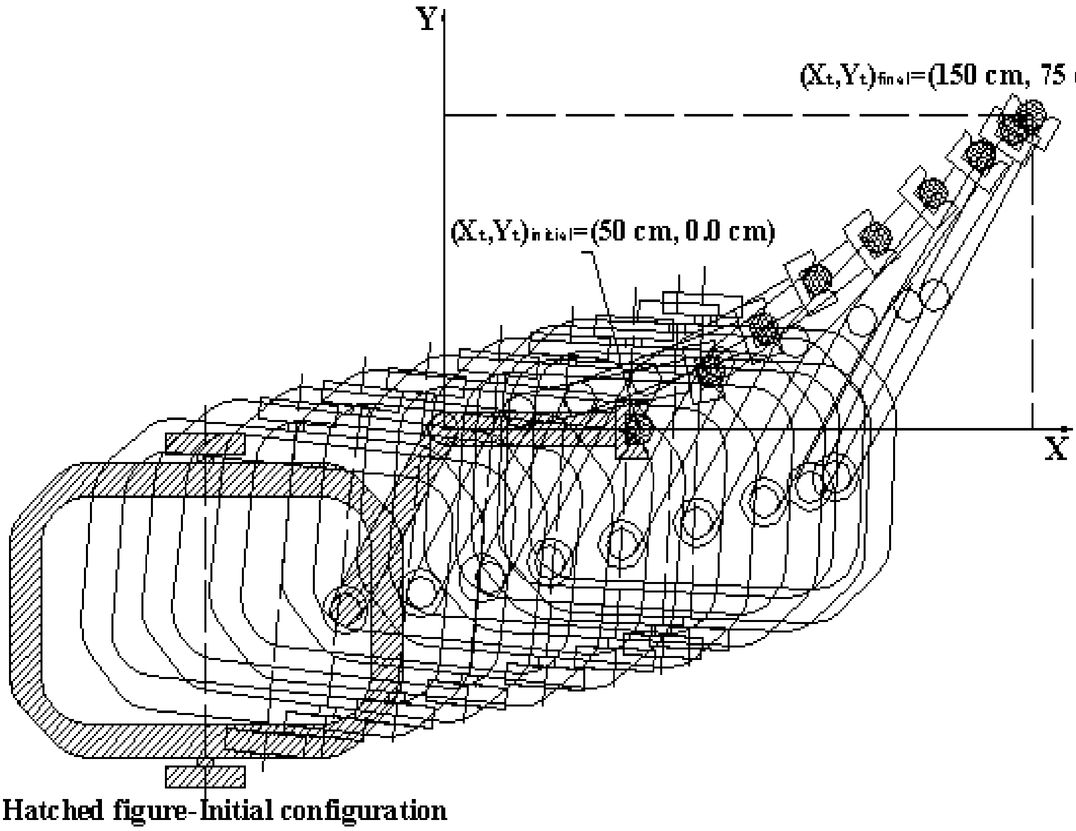

Figure 6. The movement of the mobile manipulator from initial to final configuration.

$$\tau_2 = H_{21}\ddot{X}_f + H_{22}\ddot{Y}_f + H_{23}\dot{\omega}_2 + H_{24}\dot{\omega}_1 + H_{25}\omega_1^2 \quad (28)$$

where,

$$H_{11} = -[(m_2 l_{c2} + m_l l_2)\sin(\theta_0+\theta_1+\theta_2)] + [((m_2+m_l)l_1 + m_1 l_{c1})\sin(\theta_0+\theta_1)]$$

$$H_{12} = (m_2 l_{c2} + m_l l_2)\cos(\theta_0+\theta_1+\theta_2) + ((m_2+m_l)l_1 + m_1 l_{c1})\cos(\theta_0+\theta_1)$$

$$H_{13} = {}^{c2}I + m_2 l_{c2}^2 + m_l l_2^2 - l_1(m_2 l_{c2} + m_l l_2)\cos(\theta_2)$$

$$H_{14} = -l_1(m_2 l_{c2} + m_l l_2)\sin(\theta_2)$$

$$H_{15} = {}^{c1}I + m_1 l_{c1}^2 + (m_2+m_l)l_1^2 + (m_2 l_{c2} + m_l l_2)\cos(\theta_2)$$

$$H_{16} = -l_1(m_2 l_{c2} + m_l l_2)\sin(\theta_2)$$

$$H_{21} = -(m_2 l_{c2} + m_l l_2)\sin(\theta_0+\theta_1+\theta_2)$$

$$H_{22} = (m_2 l_{c2} + m_l l_2)\cos(\theta_0+\theta_1+\theta_2)$$

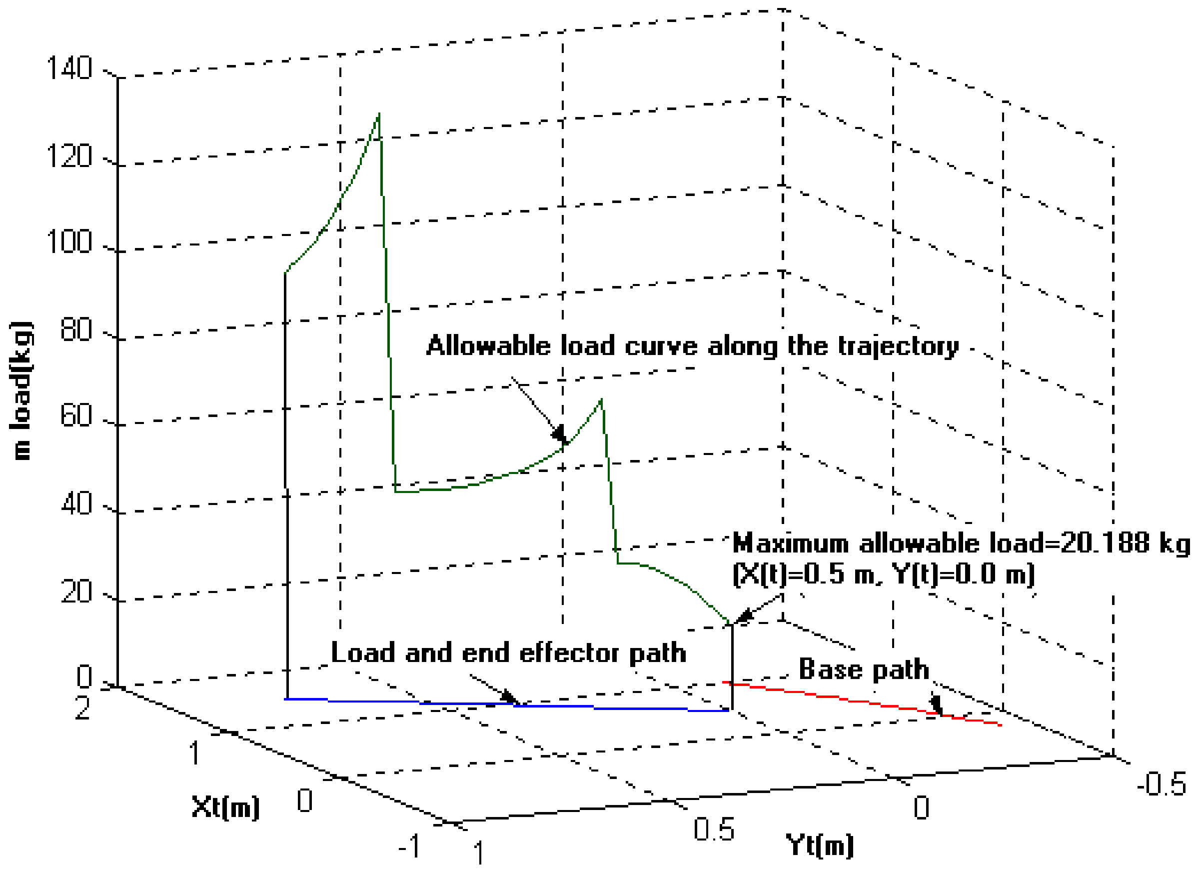

Figure 7. The variation of the allowable load along the load trajectory and associated maximum allowable load.

$$H_{23} = {}^{c2}I + m_2 l_{c2}^2 + m_l l_2^2$$

$$H_{24} = (m_2 l_{c2} + m_l l_2) l_1 \cos(\theta_2)$$

$$H_{25} = -(m_2 l_{c2} + m_l l_2) l_1 \sin(\theta_2)$$

In the above formulations $\omega_1 = \dot{\theta}_0 + \dot{\theta}_1$ and $\omega_2 = \dot{\theta}_0 + \dot{\theta}_1 + \dot{\theta}_2$ are the angular velocities of the manipulator links relative to inertial coordinate frame and l_{ci} is length of the ith link center of mass from its distal joint. The task space trajectory is discretized into equally spaced $m = 40$ points. Then by the procedure outlined in the Sec. 4 the maximum allowable load of the mobile manipulator is determined (Figure 4). The allowable load carrying capacity for the mobile manipulator at each point of trajectory is determined and maximum allowable load was found $m_{load} = 37.147kg$ at the point $x_t = 1.276m$ and $y_t = 0.612m$. Also, the corresponding base and links angles and angular velocity variations along the trajectory are illustrated in Figure 5.

5.2. Simulation Model-2 The planar mobile manipulator similar to the Case 1 is considered. The manipulator elbow angle β between two arms and end effector orientation relative to the world coordinate frame α are used as additional constraint equations. Thus

$$\begin{aligned} X_{1z} &= \beta = \pi - \theta_2 \\ X_{2z} &= \alpha = \theta_0 + \theta_1 + \theta_2 \end{aligned} \tag{29}$$

The corresponding differential kinematic equation and augmented Jacobian matrix is derived by combining the Equations (A-4), (A-5) and time derivatives of the Equation 29

$$\begin{pmatrix} Sin(\theta_0) & -Cos(\theta_0) & l_0 & 0 & 0 \\ 1 & 0 & J_{23} & J_{24} & J_{25} \\ 0 & 1 & J_{33} & J_{34} & J_{35} \\ 0 & 0 & 1 & 1 & 1 \\ 0 & 0 & 0 & 0 & -1 \end{pmatrix} \begin{pmatrix} \dot{x}_f \\ \dot{y}_f \\ \dot{\theta}_0 \\ \dot{\theta}_1 \\ \dot{\theta}_2 \end{pmatrix} = \begin{pmatrix} 0 \\ \dot{x}_e \\ \dot{y}_e \\ \dot{\alpha} \\ \dot{\beta} \end{pmatrix} \tag{30}$$

The determinant of the augmented Jacobian matrix on the left hand side of the Equation (30) is found to be $Det(J) = l_0 \neq 0$. Therefore, the matrix J is non-singular regardless of the configuration of the mobile manipulator.

The initial task vector is considered as $X_i = \{x_t, y_t, \alpha, \beta\}_i = \{50cm, 0cm, 0^\circ, 120^\circ\}$ and desired final task vector at time $t = 2Sec$ is specified as $X_f = \{x_t, y_t, \alpha, \beta\}_f = \{150cm, 75cm, 60^\circ, 180^\circ\}$

Similar to the Case 1 the final tool tip position is not attainable without the base motion. By considering straight lines from initial to final configuration for the task space variables, the overall movement of the mobile manipulator is determined and illustrated by the simulation study (Figure 6).

The task space trajectory is discretized into equally spaced $m = 40$ points. The allowable load carrying capacity for the mobile manipulator at every point of the trajectory is determined and maximum allowable load is found $m_{load} = 20.188kg$ at point $(x_t = 0.5m, \quad y_t = 0.0m)$ as shown in Figure 7.

The corresponding base and links angle and angular velocity variations along the trajectory are illustrated in Figure 8.

In the above two case studies, the same trajectory for the load is considered. However, in each case different additional kinematical constraint is considered for redundancy resolution. It is seen that load capacity of the mobile manipulator varies along its path depends on the predefined trajectory of the load. Also it can be seen, the maximum allowable load has a different value in each case. Therefore, the value of maximum allowable load for a given trajectory depends on the additional constraint functions that we apply to redundancy resolution. The type of these constraint functions directly depends on the user requirements and can be chosen arbitrarily by considering workspace limitations, obstacle avoidance or optimization criteria.

5.3. Matlab Ver 6.01 In this paper, the program MATLAB Release 12 Ver. 6.01 is used for dynamic modeling and simulation studies. This program provides many features that are useful in kinematic, dynamic and trajectory planning in robotics as well as useful capabilities for simulation analysis and results from experiments with real robots. Also there are some toolboxes and publications written by the MATLAB that provides

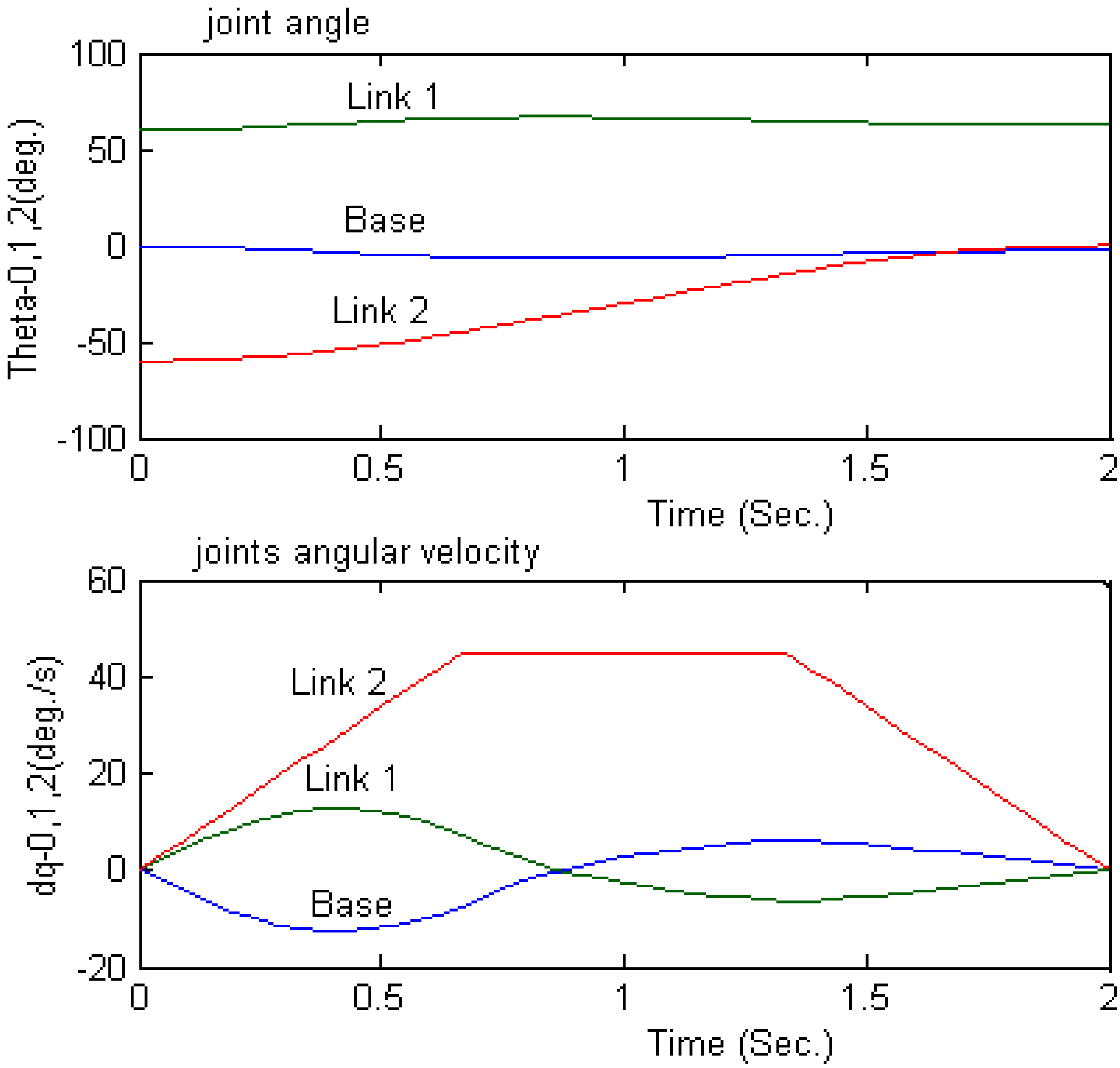

Figure 8. Variations of the base and links angles and angular velocities along the trajectory.

many functions and libraries for the kinematic and dynamic analysis of robotic manipulators [11,12].

6. CONLUSIONS

The motion planning and dynamic modeling of mobile manipulators using the augmented Jacobian technique and recursive Newton-Euler method are presented. The application of the algorithm is outlined by simulation studies in detail. In the two case studies a two-link planar differentially driven mobile manipulator with a similar trajectory for the load, and different additional constraint functions for redundancy resolution is considered. In the first case the base coordinates x_f and y_f are applied as additional constraints and corresponding maximum allowable load is computed $m_{load} = 37.147$ kg. In the second case, the angle between the two links of manipulator and angle of the end effector are considered as additional constraints and corresponding maximum allowable load is computed as $m_{load} = 20.188$ kg. Hence, the results of the case studies are shown that the allowable load is variable along the given trajectory. Also in mobile manipulators in contrast with the fixed base manipulators, the maximum allowable load on a given trajectory has not a unique value. But, a special and unique value may be computed depends on the type of the applied additional constraint functions to resolve the redundancy resolution.

APPENDIX A.

A.1. Case 1 Kinematics The coordinate of the end effector with respect to joint variables θ_0, θ_1 and θ_2 is

$$\begin{aligned} x_e &= x_f + l_1 \cos(\theta_0 + \theta_1) + l_2 \cos(\theta_0 + \theta_1 + \theta_2) \\ y_e &= y_f + l_1 \sin(\theta_0 + \theta_1) + l_2 \sin(\theta_0 + \theta_1 + \theta_2) \end{aligned} \tag{A-1}$$

As explained in Section 5.1 the user specified additional constraints are considered as the base position coordinates

$$\begin{aligned} X_{1z} &= x_f \\ X_{2z} &= y_f \end{aligned} \tag{A-2}$$

by differentiating of Equations (A-2) with respect to time we have:

$$\begin{aligned} \dot{X}_{1z} &= \dot{x}_f \\ \dot{X}_{2z} &= \dot{y}_f \end{aligned} \tag{A-3}$$

We assume that the speed at which the system moves is low and therefore the two driven wheels do not sleep sideways. The nonholonomic constraint equation for the manipulator attachment point F :

$$\dot{x}_f \sin(\theta_0) - \dot{y}_f \cos(\theta_0) + \dot{\theta}_0 l_0 = 0 \tag{A-4}$$

where l_0 is the distance between platform center of mass G and point F (Figure 2). By differentiating Equation (A-1), the end effector velocity components are as below

$$\begin{aligned} \dot{x}_e &= \dot{x}_f - l_1(\dot{\theta}_0 + \dot{\theta}_1)\sin(\theta_0 + \theta_1) - \\ &\quad l_2(\dot{\theta}_0 + \dot{\theta}_1 + \dot{\theta}_2)\sin(\theta_0 + \theta_1 + \theta_2) \\ \dot{y}_e &= \dot{y}_f + l_1(\dot{\theta}_0 + \dot{\theta}_1)\cos(\theta_0 + \theta_1) + \\ &\quad l_2(\dot{\theta}_0 + \dot{\theta}_1 + \dot{\theta}_2)\cos(\theta_0 + \theta_1 + \theta_2) \end{aligned} \tag{A-5}$$

In the inverse kinematics problem, we find θ_1 and θ_2 which correspond to a given load position (x_e, y_e) and a given platform position (x_f, y_f).

The angle θ_2 is found by the following expression

$$\theta_2 = Arc\cos\left(((x_e - x_f)^2 + (y_e - y_f)^2 - l_1^2 - l_2^2) \Big/ 2l_1 l_2 \right) \tag{A-6}$$

By discretizing the robot trajectory into m points and by numerical integration of Equation (A-4) The angle θ_0 can be found. The variables $\dot{x}_f$ and $\dot{y}_f$ are known, therefore

$$\begin{aligned} &\theta_0(i+1) = \theta_0(i) + (\dot{y}_f(i)\cos(\theta_0(i)) - \\ &\dot{x}_f(i)\sin(\theta_0(i)) \times dt / l_0 = 0 \end{aligned} \tag{A-7}$$

where $i = 1 \quad to \quad m$ and $dt = T_{total} / m$.

Similarly, the angle θ_1 is given by

$$\theta_1 = Arc\cos\left(\frac{\left((l_1 + l_2 \cos(\theta_2))(x_e - x_f) - l_2 \sin(\theta_2)(y_e - y_f)\right)}{(x_e - x_f)^2 + (y_e - y_f)^2}\right) - \theta_0 \tag{A-8}$$

A.2. Case 2 Kinematics As explained in Section 5.2 the user specified additional constraints are:

$$X_{1z} = \beta = \pi - \theta_2 \quad and \quad X_{2z} = \alpha = \theta_0 + \theta_1 + \theta_2 \tag{A-9}$$

In this case, the inverse kinematic of the system is derived as bellow

$$\theta_2 = \pi - \beta \tag{A-10}$$

Similar to the Case 1 the base angle relative to the world coordinate frame θ_0 numerically can be computed by using the Equation (A-7). The angle of the manipulator first link relative to the base main axis θ_1 by using the second part of the Equation (A-9) can be calculated as bellow

$$\theta_1 = \alpha - (\theta_0 + \theta_2) \tag{A-11}$$

The base position relative to world coordinate frame at point F is calculated by rearranging Equation (A-1). Therefore we have

$$x_f = \mathrm{x_e} - l_1 \cos(\theta_0 + \theta_1) - l_2 \cos(\alpha)$$
$$y_f = y_e - l_1 \sin(\theta_0 + \theta_1) - l_2 \sin(\alpha) \tag{A-12}$$

7. REFERENCES

1. Wang, L. T. and Ravani, B., "Dynamic Load Carrying Capacity of Mechanical Manipulators-Part 1: Problem Formulation", ***J. of Dyn. Sys. Meas. and Control***, Vol. 110, (1988), 46-52.
2. Yao, Y. L., Korayem, M. H. and Basu, A., "Maximum Allowable Load of Flexible Manipulators for a Given Dynamic Trajectory", ***Robotics and Computer-Integrated Manufacturing***, Vol. 10, No. 4, (1993), 301-309.
3. Korayem, M. H. and Basu, A., "Formulation and Numerical Solution of Elastic Robot Dynamic Motion with Maximum Load Carrying Capacity", ***Robotica***, Vol. 12, (1994), 253-261.
4. Korayem, M. H. and Basu, A. "Dynamic Load Carrying Capacity for Robotic Manipulators with Joint Elasticity Imposing Accuracy Constraints", ***Robotic and Autonomous Systems***, Vol. 13, (1994), 219-229.
5. Carriker et al., W. F., "The Use of Simulated Annealing to Solve the Mobile Manipulator Path Planning Problem", ***Proc. of IEEE Int. Conf. on Rob. and Autom***, (1992), 204-209.
6. Papadopoulos, E. G. and Gonthier, Y., "A Frame Force for Large Force Task Planning of Mobile and Redundant Manipulators", ***J. of Robotic Systems***, Vol. 16, No.3, (1999), 151-162.
7. Papadopoulos, E. G. and Ray, D. R., "A New Measure of Tip Over Stability Margin for Mobile Manipulators", ***Proc. of IEEE Int. Conf. on Rob. and Autom.***, (1996), 3111-3116.
8. Ghasempoor, A. and Sepehri, N., "A Measure of Stability for Mobile Based Manipulators", ***Proc. of IEEE Int. Conf. on Rob. and Autom***, (1995), 2249-2254.
9. Ray, D. A. and Papadopoulos, E. G., "Online Automatic Tip-Over Preventation for Mobile and Redundant Manipulators", ***J. of Robotic Systems***, Vol. 16, No. 3, (1999), 151-162.
10. Ghariblu, H. and Korayem, M. H., "Mathematical Analysis of Kinematic Redundancy and Constraints on Robotic Mobile Manipulators", ***Second International Conference of Applied Mathematics***, Tehran, (2000), 502-511.
11. Corke, P. I., "Robotic Toolbox for MATLAB", ***Manufacturing Science and Technology***, Pinjarra Hills, Australia, (2001).
12. Legani et. al., G., "SPACELIB in MATLAB User's Manual", University of Brescia-Mechanical Engineering Department, (July 1998).